ELSEVIER

Titanium–halide catalyst-precursors in sodium aluminum hydrides

E.H. Majzoub*, K.J. Gross

Sandia National Laboratories, Analytical Materials Science Department, P.O. Box 969, Livermore, CA 94551, USA
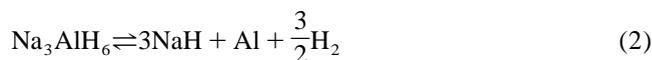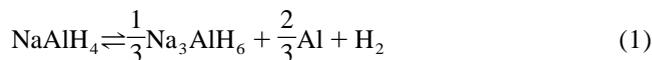
Abstract

The kinetics of absorption and desorption of hydrogen from $NaAlH_4$ have previously been shown to improve upon the addition of a catalyst-precursor such as $TiCl_3$. In this paper we demonstrate that $TiCl_2$, TiF_3, and $TiBr_4$ all effectively improve sorption kinetics. Arrhenius data indicate that the catalyst precursors behave in essentially the same manner. Evidently the valency of Ti in the catalyst-precursor is inconsequential to the role of Ti in altering the kinetic mechanism. The formation of $TiAl_3$ on doping with $TiCl_3$ has been observed. The presence of $TiAl_3$ appears to contribute in part to the enhanced kinetics in these systems.
© 2003 Elsevier B.V. All rights reserved.

1. Introduction

Sodium aluminum tetrahydride decomposes in two steps, first into the hexahydride Na_3AlH_6, which further decomposes into NaH as follows

$$NaAlH_4 \rightleftharpoons \frac{1}{3}Na_3AlH_6 + \frac{2}{3}Al + H_2 \qquad (1)$$

$$Na_3AlH_6 \rightleftharpoons 3NaH + Al + \frac{3}{2}H_2 \qquad (2)$$

This system was shown to be reversible by Bogdanović et al. upon doping with various transition metal catalysts [1]. Speculation about the effect of the catalyst-precursor has led to suggestions that Ti^{3+} plays an active role in enhancing the kinetics of absorption and desorption [2,3]. Therefore several Ti–halide compounds of differing valency were chosen as catalyst-precursors. These were $TiCl_3$, $TiCl_2$, TiF_3, and $TiBr_4$. Samples were prepared for each dopant and tested for reversible hydrogen capacity. The desorption rates were measured as a function of temperature, and Arrhenius analysis was applied. The Gibbs free energies of formation for the reactions of dopant and pre-active material are evaluated with respect to the observed desorption rate data. The primary goals of this work are to determine (1) if the valency of the

Ti-precursor is of any importance, (2) if there is any correlation between the reactivity of the Ti–halide catalyst-precursor and the resulting rate kinetics, and (3) if $TiAl_3$ is responsible for enhancing kinetics.

The lighter Ti–halides $TiCl_2$ and TiF_3 were also chosen to increase the weight percent of hydrogen capacity in the doped material. Assuming the reactions in Eqs. (1) and (2) go to completion, there are three hydrogen atoms per formula unit available for absorption and desorption. Capacity as a function of catalyst loading can be easily calculated for various Ti–halide combinations. The limiting value of the reversible hydrogen weight capacity in the $NaAlH_4$ system is 5.55%, in the limit that the catalyst loading approaches zero. Values for the total weight percent of reversible hydrogen, under ideal conditions, for the dopants used here are given in Fig. 1 for samples of composition $(1 + xy/100)NaAlH_4 + xTi(halide)_y$.

2. Experimental details

Active $NaAlH_4$ material was prepared from NaH (99.99%) and 20 μm Al (99.99%) powder purchased from Sigma–Aldrich using a direct synthesis method [4]. Typically a 7-g mixture of 1:1:0.04 molar ratio of NaH:Al: catalyst-precursor was mechanically milled in a SPEX 8000 high energy mill using a WC milling pod and 6–9 25-g WC balls. The catalyst-precursor consisted of Ti–halide such as $TiCl_3$, TiF_3, $TiCl_2$, and $TiBr_4$, purchased

*Corresponding author. Tel.: +1-925-294-2498; fax: +1-925-294-3410.
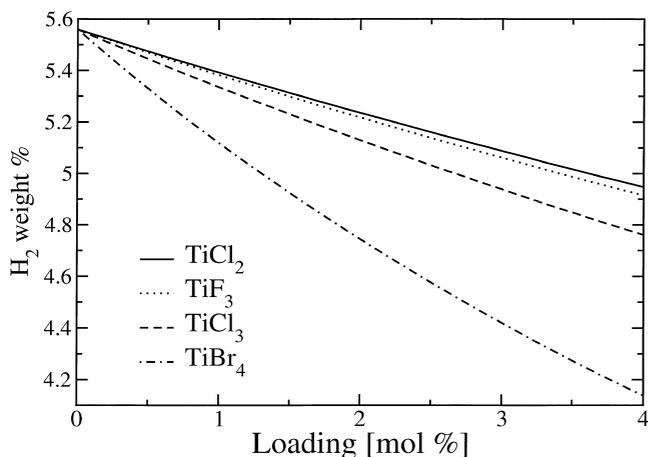
E-mail address: ehmajzo@sandia.gov (E.H. Majzoub).

Fig. 1. Ideal hydrogen weight percent capacity with catalyst-precursor loading for the Ti–halides used in this work.

from Sigma–Aldrich. Sample sizes of about 2 g were transferred to a sealed stainless-steel sample vessel and connected to a pressure- and temperature-controlled hydrogen manifold. All steps for sample preparation and transfer into the reactor vessel occurred inside an Ar glove box with oxygen levels below 3 ppm.

Samples from earlier work were prepared from $NaAlH_4$ which was precipitated from a 1 M solution in tetrahydrofuran (THF) by vacuum evaporation [5]. For some comparisons, those samples are labeled THF-derived (THF) to distinguish them from the direct synthesis (DS) samples in this work.

Kinetics of absorption and desorption were determined from pressure measurements in a calibrated fixed-volume apparatus. Samples were placed in a 15-mm-diameter 316SS vessel of ~12 cc volume with a 1-mm-diameter internal thermocouple well for rapid response of the material during kinetics experiments. Type K thermocouples with a temperature resolution of 0.1 K were placed at the top, middle, and bottom of the sample location on the exterior of the containment tube, and inside the thermocouple well near the center of the sample. The sample was held in place on the top and the bottom with Fiberfax glass fiber. Absorption measurements were made in a calibrated volume of 120 cc at pressures around 10 MPa. For a 2 g sample of $NaAlH_4$, this resulted in a pressure drop of around 0.8 MPa. Absorption pressures were measured using a Teledyne Taber model 206 piezoelectric transducer with a resolution of 10^{-2} MPa. Measured values of (mol H)/(mol Al) have a resolution of about ±0.2. The volume used for the desorption measurements was about 1040 cc, and the pressure was measured using a Baratron capacitance manometer with a resolution of 10^{-7} MPa. The sample temperature was regulated with an Omega model CN76000 PID controller connected to heating tape wrapped around the exterior of the SS vessel. Typical absorption parameters were 120 °C and 8.5 MPa hydrogen overpressure. Desorptions were performed in an initial
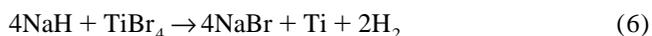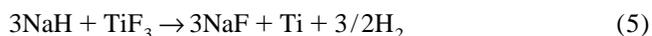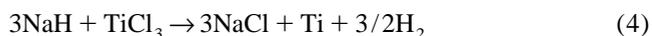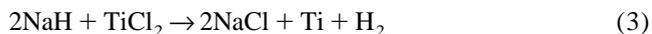
vacuum of 1 Torr while increasing the temperature in steps to determine Arrhenius behaviour.

$TiAl_3$ in the $L1_2$ structure was prepared by mechanically milling Alpha Products 100 mesh Ti (99.9%), and Aldrich 635 mesh Al (99.9%), in a 1:3 molar ratio for 24 h.

Samples were characterized for hydride-phase content following absorption and desorption cycles using Cu Kα radiation on a Scintag XDS-2000 using Bragg–Brentano geometry and airless sample holders.

3. Results and discussion

Sodium halide salts form in the doping process due to the reactions below.

$$2NaH + TiCl_2 \rightarrow 2NaCl + Ti + H_2 \qquad (3)$$

$$3NaH + TiCl_3 \rightarrow 3NaCl + Ti + 3/2H_2 \qquad (4)$$

$$3NaH + TiF_3 \rightarrow 3NaF + Ti + 3/2H_2 \qquad (5)$$

$$4NaH + TiBr_4 \rightarrow 4NaBr + Ti + 2H_2 \qquad (6)$$

The resultant form of the titanium is shown as metallic, but may form a reaction product itself and will be discussed in the next section. Bulk Ti has never been observed in our diffraction data.

The halide salts produced in these reactions add additional weight of inactive material, resulting in two effects. (1) It causes a significant reduction in the overall reversible hydrogen capacity of the material. (2) It necessitates the comparison of capacities on an 'active material' basis. This makes it desirable to plot capacities of the post-doped material as (mol H)/(mol Na) versus the at.% doping level, where the moles of Na are those not bound in Na–halide. This eliminates the weight of the inactive material component. We represent this quantity as H/Na_a (representing the 'active' Na available) which should have a maximum value of 3. This allows us to determine the extent of the reversibility of the reactions. Values for H/Na_a are shown for second desorptions for several samples in Fig. 2.

The reference $NaAlH_4$ sample (only desorbed once) labeled 'no catalyst' was prepared from THF and mechanically milled, resulting in a small loss of capacity. Clearly, the Ti-doped samples are not entirely reversible, whether they were prepared from THF alanate or by the direct synthesis method, which generally show lower H/Na_a values. This loss in reversibility is perhaps due to phase separation induced during cycling and the inability of aluminum to diffuse quickly enough during absorptions, thus leading to deficient desorptions. Crystalline aluminum can be seen in the X-ray of a post fourth absorption of TiF_3-doped material as shown in Fig. 3. In situ studies have demonstrated that aluminum precipitates to form crystallites during desorption [6,7].

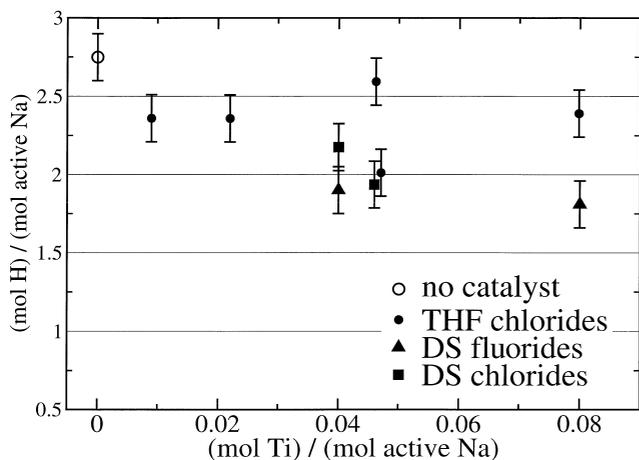Arrhenius data for the rates of decomposition of the

Fig. 2. Capacity of Ti–halide doped material for 2nd desorptions. The maximum value of 3 represents the total number of hydrogens per formula unit which should participate in the absorption/desorption reactions.

Fig. 4. Arrhenius plot of the rates of desorption of tetrahydride for samples using Ti–halide catalyst-precursors.

tetrahydride are shown in Fig. 4 for each of the Ti–halide catalyst precursors. These data indicate that all the Ti–halides behave in essentially the same manner with the desorption rates in the order of highest to lowest corresponding to the dopants $TiCl_2$, $TiCl_3$, TiF_3, $TiBr_4$. Note that the $TiBr_4$ sample had a lower doping level (1.4 at.%) and a slightly lower desorption rate, consistent with results obtained by Sandrock et al. [5]. The 'no catalyst' sample prepared from THF is shown as a comparison.

The Gibbs free energies of the reactions (3)–(6) are shown in Table 1 and indicate that the order of the most exothermic to least exothermic reaction is in the order $TiCl_3$, $TiBr_4$, $TiCl_2$, TiF_3. Yet the $TiCl_2$-doped sample yields the best kinetics. Therefore, the free energy of reaction does not seem to be correlated with the enhancement of sorption kinetics. However, doping with Ti powder alone, in which there is no large enthalpy of
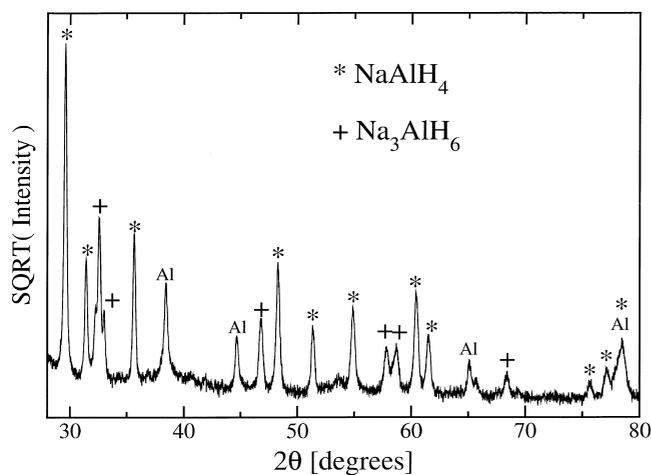
reaction, produces samples with nearly no improvement in kinetics over two cycles. The system behaves almost undoped, and it appears that the halide component is necessary for obtaining active samples. Thus the very exothermic reaction with the Ti–halides seems to atomically disperse the Ti, since it is apparently unfavorable, energetically, to remove it from bulk Ti when doping with this material. Ti doping with other non-halide materials can, however, show enhancement of kinetics [8]. Assuming that the titanium is atomically dispersed as a substitute ion in the bulk of NaH in the desorbed state, or in $NaAlH_4$ in the absorbed state, its charge state is expectedly independent of its precursor valency and thus all halide dopants show similar kinetic effects as indicated in Fig. 4.

3.1. Titanium compounds

The product titanium in Eqs. (3)–(6) may, however, form a hydride or Ti–Al alloys. The free energy of formation, ΔG_f°, for Eq. (4) is −398 kJ/mol, if the resultant Ti is metallic. If we assume the Ti forms TiH_2 or $TiAl_3$, the resulting reactions are

$$3NaH + TiCl_3 \rightarrow 3NaCl + 1/2H_2 + TiH_2 \quad (7)$$

$$3NaH + 3Al + TiCl_3 \rightarrow 3NaCl + TiAl_3 + 3/2H_2 \quad (8)$$

with free energies of formation of −484 kJ/mol, and

Fig. 3. X-ray powder diffraction of post 4th absorption of a sample prepared from NaH, Al, TiF_3. The presence of hexahydride and free aluminum indicate that the reverse reaction (Eq. (2)) is incomplete.
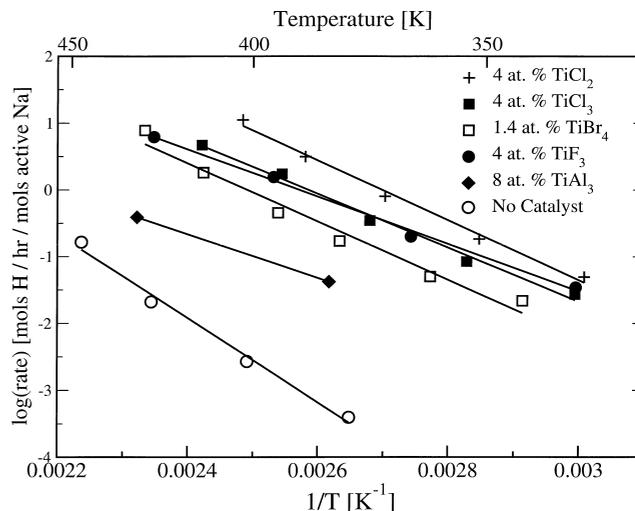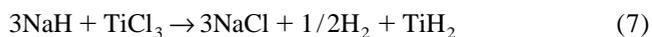
Table 1
Gibbs free energies of formation for the reactions in Eqs. (3)–(6)

Compound	Equation	ΔG_f° (kJ/mol)
$TiCl_2$	(3)	−236.8
$TiCl_3$	(4)	−398.3
TiF_3	(5)	−176.5
$TiBr_4$	(6)	−323.5

−535 kJ/mol, respectively. This difference results from the energy of formation for TiH_2 (−86 kJ/mol [9]), or $TiAl_3$ (−136 kJ/mol [10]). The value of ΔG_f° for TiAl is −72 kJ/mol, which is lower in magnitude than that for TiH_2 and is ignored. This suggests that the formation of $TiAl_3$ is preferred. Due to the small volume fraction of the phases that would be present, X-ray diffraction of the doped material was inconclusive on the presence of TiH_2 or $TiAl_3$ in these (DS) materials. However, favorable stoichiometry is achieved for $TiAl_3$ formation with the use of $TiCl_3$ as a dopant and its presence is indicated in the $LiAlH_4$ system, where micro-crystalline $TiAl_3$ is thought to act as a heterogeneous dehydrogenation catalyst after reacting with $TiCl_4$ [11].

To investigate the formation of $TiAl_3$ in the $NaAlH_4$ system, a mechanically milled 3:1 mixture of $NaAlH_4$ and $TiCl_3$ was prepared. X-ray diffraction indicates the formation of NaCl and $TiAl_3$ in the $L1_2$ structure, as shown in Fig. 5 and is consistent with the following reaction

$$TiCl_3 + 3NaAlH_4 \rightarrow 3NaCl + TiAl_3 + 6H_2 \qquad (9)$$
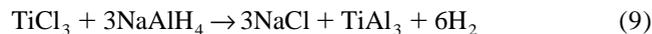
The presence of $TiAl_3$ contributes to the broad peak widths of the reacted sample peaks at 45, 65, and 80 degrees 2θ. Scherrer analysis of the $L1_2$ phase peak widths shown in Fig. 5 for the pure $TiAl_3$ pattern place an upper limit on the coherence length of about 7 nm. The NaCl peaks which are not overlapping with $TiAl_3$, at 56 and 75 degrees 2θ, have peak widths corresponding to a coherence length of about 25 nm. The 3:1 mixture of $NaAlH_4$ and $TiCl_3$ corresponds to a doping level of 33 mol.%. At doping levels of 4 mol.%, it is difficult to observe the presence of the $L1_2$ phase in X-ray diffraction due to the large peak widths and small volume fraction of the phase. To investigate the kinetic effect of doping with $TiAl_3$, a small
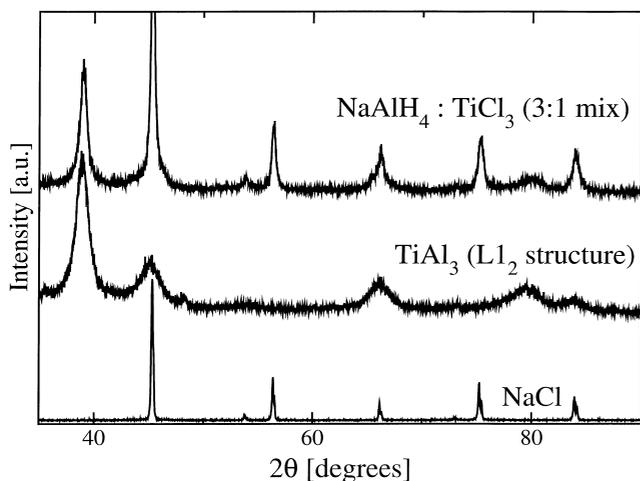
amount of $TiAl_3$ was prepared by mechanical alloying and added without Ti–halide to the direct synthesis material. The doping procedure was identical to that of the Ti–halides. The desorption kinetics of 8 mol.% $L1_2$-doped material are an order of magnitude below those of Ti–halide-doped samples (see Fig. 4). This suggests that if formation of $TiAl_3$ occurs in the 4 mol.% doped Ti–halide samples, it is not the only mechanism responsible for enhancing the sorption kinetics. It may be possible that during ball milling Ti is removed from $TiAl_3$ and is available for incorporation into the alanate. This would be consistent with recent results on doping with TiH_2, which indicate that Ti can be removed from this relatively stable compound and participate in kinetics enhancement [8]. There is also the small possibility that the addition of $TiAl_3$ may act only as a grinding aid, similar to the results obtained by using carbon as a milling ingredient [12]. Therefore, if the Ti is not in $TiAl_3$ and the sorption kinetics are significantly enhanced, the high absolute activity of the Ti resulting from the strongly exothermic reactions (3)–(6), and the relatively low mol.% doping level suggest that the titanium is left as a substitute ion in the system.

4. Conclusions

The enhanced sorption kinetics due to Ti–halide catalyst precursors is independent of the valence state of the Ti–halide, and the data indicate that the more exothermic halides do not result in faster rate kinetics. The free energies of formation suggest that $TiAl_3$ is the most likely reaction product. The presence of $TiAl_3$ alone, however, cannot explain the sorption kinetics of doped sodium aluminum hydride. This suggests that the Ti is atomically dispersed in the system, both as a substitute ion and perhaps in $TiAl_3$, by the very exothermic formation of Na–halide. This conclusion is consistent with recent X-ray diffraction studies suggesting that Ti may be substituting into bulk $NaAlH_4$ [3]. Because the sorption kinetics are similar for the Ti–halide dopants, if the titanium is substituted in the $NaAlH_4$, or Na_3AlH_6, it is reasonable that its resulting charge state will be independent of the catalyst-precursor used.

Fig. 5. X-ray diffraction indicating $TiAl_3$ production in the $NaAlH_4$ system when mechanically milled in a 3:1 ratio with $TiCl_3$.

References

[1] B. Bogdanović, R.A. Brand, A. Marjanovic, M. Schwickardi, J. Tolle, Metal-doped sodium aluminium hydrides as potential new hydrogen storage materials, J. Alloys Comp. 302 (1–2) (2000) 36–58.

[2] C.M. Jensen, R. Zidan, N. Mariels, A. Hee, C. Hagen, Advanced titanium doping of sodium aluminum hydride: segue to a practical hydrogen storage material?, Int. J. Hydrogen Energy 24 (5) (1999) 461–465.

[3] D. Sun, T. Kiyobayashi, H.T. Takeshita, N. Kuriyama, C.M. Jensen, X-ray diffraction studies of titanium and zirconium doped NaAlH$_4$: elucidation of doping induced structural changes and their relationship to enhanced hydrogen storage properties, J. Alloys Comp. 337 (2002) L8–L11.

[4] K.J. Gross, E.H. Majzoub, Direct synthesis of light-weight catalyzed hydride for hydrogen storage, United States patent application submitted 2002.

[5] G. Sandrock, K. Gross, G. Thomas, C. Jensen, D. Meeker, S. Takara, Engineering considerations in the use of catalyzed sodium alanates for hydrogen storage, J. Alloys Comp. 330–332 (2002) 696–701.

[6] K.J. Gross, G. Sandrock, G.J. Thomas, Dynamic in situ X-ray diffraction of catalyzed alanates, J. Alloys Comp. 330–332 (2002) 691–695.

[7] K.J. Gross, S. Guthrie, S. Takara, G. Thomas, In-situ X-ray diffraction study of the decomposition of NaAlH$_4$, J. Alloys Comp. 297 (1–2) (2000) 270–281.

[8] K.J. Gross, E.H. Majzoub, S.W. Spangler, Hydrogen absorption properties of alanates: from principle to practice. International Conference on Metal Hydrogen Systems, Annecy, France (2002) submitted.

[9] W.M. Mueller, J.P. Blackledge, G.G. Libowitz, Metal Hydrides, Academic Press, New York, 1968.

[10] C.J. Smithells, G.B. Brook, E.A. Brandes (Eds.), 7th Edition, Smithells Metals Reference Book, Butterworth–Heinemann, 1998.

[11] V.P. Balema, J.W. Wiench, K.W. Dennis, M. Pruski, V. Pecharsky, Titanium catalyzed solid-state transformations in LiAlH$_4$ during high-energy ball-milling, J. Alloys Comp. 329 (2001) 108–114.

[12] A. Zaluska, L. Zaluski, J.O. Strom-Olsen, Sodium alanates for reversible hydrogen storage, J. Alloys Comp. 298 (1–2) (2000) 125–134.